Concentration Polarization in Translocation of DNA through Nanopores and Nanochannels

Siddhartha Das,[1] Pavel Dubsky,[2] Albert van den Berg,[2] and J. C. T. Eijkel[2]

[1]*Physics of Fluids Group and J. M. Burgers Centre for Fluid Dynamics, University of Twente, P.O. Box 217, 7500 AE Enschede, The Netherlands*

[2]*BIOS, The Lab-on-a-Chip Group, MESA+ Institute for Nanotechnology, University of Twente, P.O. Box 217, 7500 AE Enschede, The Netherlands*

(Received 7 September 2011; published 26 March 2012)

In this Letter we provide a theory to show that high-field electrokinetic translocation of DNA through nanopores or nanochannels causes large transient variations of the ionic concentrations in front and at the back of the DNA due to concentration polarization (CP). The CP causes strong local conductivity variations, which can successfully explain the nontrivial current transients and ionic distributions observed in molecular dynamics simulations of nanopore DNA translocations as well as the transient current dips and spikes measured for translocating hairpin DNA. Most importantly, as the future of sequencing of DNA by nanopore translocation will be based on time-varying electrical conductance, CP, must be considered in experimental design and interpretation—currently these studies are mostly based on the incomplete pore conductance models that ignore CP and transients in the electrical conductance.

DOI: 10.1103/PhysRevLett.108.138101 PACS numbers: 87.14.gk, 87.15.Tt, 87.16.dp

Over the past few years, studies of DNA dynamics in nanopores and nanochannels in the presence of applied electric fields have received a great deal of attention, owing to their possible applications for rapid DNA sequencing and enhanced separation [1–3]. Ambiguity can arise when the nanoconfined DNA molecule is subjected to large electric fields. For example, Aksimentiev and co-workers [4] demonstrated both an increase and a decrease of current when a hairpin DNA (HP DNA) molecule translocates through a nanopore at electric field strengths of the order of 10^8 V/m [4,5]. Salieb-Beugelaar *et al.* [6] observed that the mobility of a DNA molecule confined in a nanochannel decreased rapidly at fields above 5×10^4 V/m. In this Letter we shall demonstrate for the first time that at such large fields, or equivalently large current densities, substantially strong Concentration Polarization (CP) will occur. CP classically occurs at locations of sudden local change of ionic current transport numbers, e.g., in membranes [7] or micro-nanochannel junctions [8], in presence of external electric fields. Here, the presence of nanoconfined DNA causes a sudden local change in transport numbers due to the ionic composition of its electrical double layer (EDL). An EDL is formed when an ionic solution comes in contact with a charged substrate and is characterized by a charge imbalance (which nullifies the substrate charge). Here we show that CP will occur at the opposite ends of a nanoconfined electrophoreting DNA molecule [see Figs. 1(a) and 1(c)] because the electrical double layer (EDL) formed around the DNA induces ionic concentration differences between the planes with and without the DNA molecule [planes 3 and 4 and planes 1 and 2 in Figs. 1(a) and 1(c)]. The resulting transport number differences result in CP-induced ion-depleted and ion-enriched zones in front and at the back of the translocating DNA [see Figs. 1(a) and 1(c)]. Most importantly, this causes transient changes of the conductance of the nanopore through which the DNA translocates. Future nanopore-based sequencing will require conductivity data having sufficient spatiotemporal resolution to allow single base (pair) resolution [9,10]—in this light CP will be extremely relevant as it causes strong local decreases (due to ion depletion) and increases (due to ion accumulation) in the pore conductance during the entrance and the exit phases of the DNA. This effect is not captured by the existing steady state pore conductance models [11].

At present the pore conductivity is obtained from the trans-pore current signatures at constant potential, which are modulated by the DNA pore blockage in combination with, as we will show here, transient axial concentration changes. The DNA entrance and exit phases typically last 0.1–100 μs [12], determined by translocation velocities of 0.1–100 mm/s and pore lengths of 10 nm. Since the experimental current resolution is typically limited to 10 kHz [12], single base (pair) sequencing as well as the observation of the CP-induced transients have not yet been possible. As stated by Branton *et al.* [10], for single base-pair resolution the translocation speed will have to be drastically reduced. The applied field, however, should not be reduced to ensure that one gets a measurable current. Such a combination of slow translocation and high field will, as we shall demonstrate, exacerbate CP and therefore make it highly significant for the design of future conductivity-based sequencing.

In experiments with hair pin (HP) DNA, where current signatures last several seconds, current enhancements above the open-pore current are routinely observed and hypothesized as a result of the modulation of the current

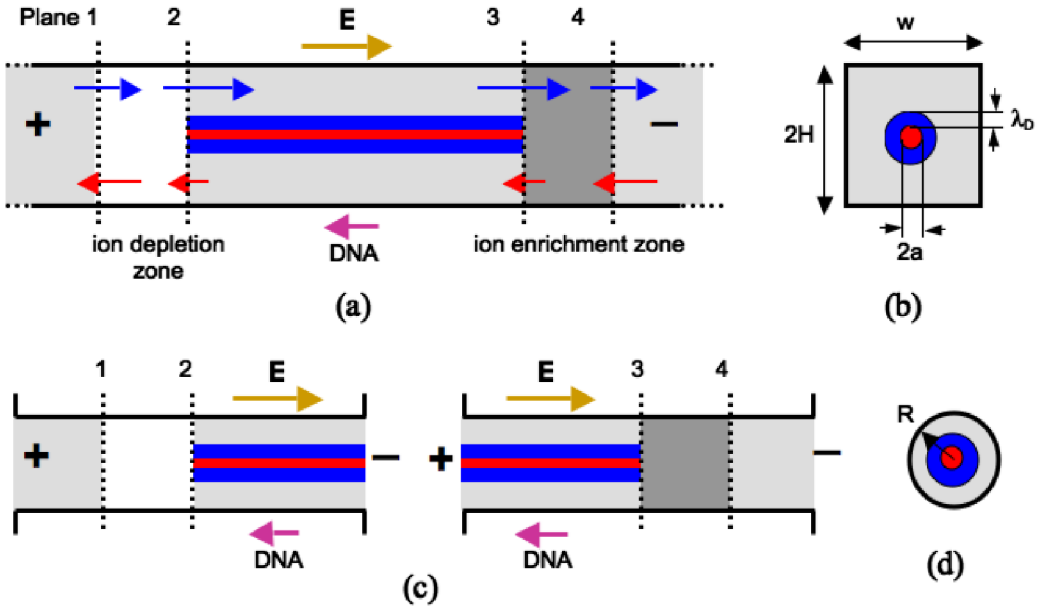

FIG. 1 (color online). (a) Schematic of DNA (in red) with a surrounding EDL (in blue) in a nanochannel, and the location of the CP-induced ion-depletion (between planes 1 and 2) and ion-enrichment (between planes 3 and 4) zones. The arrows (in blue) depicting the cationic current are located inside the nanochannel and are directed from left to right, whereas the arrows (in red) depicting the anionic current are located inside the nanochannel and are directed from right to left. (b) The different dimensions corresponding to the DNA transport in a nanochannel. The channel height is $2H$ and width w ($2H = w$), a is the DNA radius of cross section and λ_D is the DNA-EDL thickness. (c) (left) Schematic of the event of a DNA entering a nanopore (radius R) [also see Figs. 6(a),(b) in [9]], and the locations of the planes 1 and 2 in between which ion depletion will occur. (c) (right) Schematic of the event of a DNA (shown in red) exiting a nanopore [also see Figs. 6(d),(e) in [9]], and the locations of the planes 3 and 4 in between which ion enrichment will occur. (d) The different dimensions corresponding to the DNA translocation in a nanopore, having radius R. In each figure, the purple arrow (located outside the nanochannel or nanopore, and directed from right to left) denotes the direction of movement of the DNA molecule and the brown arrow (located outside the nanochannel or nanopore, and directed from left to right) denotes the direction of the applied electric field (denoted as E). Not shown for sake of clarity are EDLs at the pore or channel walls of thicknesses identical to the DNA-EDL thickness.

caused by the alteration of the DNA molecular configuration relative to the pore [4,5]. Molecular dynamics simulation studies, which, unlike experiments, do provide sufficient time resolution, demonstrate that in addition to the expected current modulations, there occurs substantial ionic depletion and accumulation at the HP DNA extremities [3,4,9]. Also molecular dynamics simulation studies for normal ds-DNA nanopore translocation have shown a post-translation current peak, which has been ascribed to a possible release of ions accumulated at the exit [12]. Our theory provides the first simple concrete explanation for both of these apparently puzzling phenomena, underlining the importance of considering CP effects in nanopore DNA translocation. In an alternative description, our proposed system of a nanopore with a translocating DNA behaves as a transient nanofluidic diode closed at the DNA entrance and open at the DNA exit [13].

We would like to emphasize that the present theory employs a continuum-based treatment. It is assumed that the atomistic effects can be averaged and the inhomogeneity of the system may be represented by Manning condensation and classical EDL theory. This is equivalent to the assumptions made by Smeets *et al.* [11] for DNA pore translocation. Also, we do not consider electroosmotic flow—this is justified since electroosmosis will affect the movement of the DNA and the dissolved ions in equal measure, and will hence not affect CP development. We furthermore assume that the entire event of CP and its associated effects develop over a time scale ($\sim$ 10 ns, see Fig. 4) which is substantially smaller than the DNA electromigration time scale (either in nanochannel or nanopore) ($\sim$ 0.1–100 μs), and accordingly all the calculations effectively consider the DNA as a static body with finite negative charge.

We start by considering a simplified picture, where a single stationary DNA molecule is confined in a nanochannel of height $2H$ and width w (or entering or exiting a nanopore of radius R, with the nanopore being shorter in length than the DNA molecule) and is sufficiently stretched to be considered in a cylindrical conformation [see Figs. 1(a) and 1(c)]. We consider identical ionic current densities, i.e., $j_1 = j_{1,+} + j_{1,-} = j_2 = j_{2,+} + j_{2,-} = j$ at the planes 1 and 2 [plane 2 contains the DNA EDL, whereas plane 1 is far away from it, see Figs. 1(a) and 1(c); note that exactly equivalent analysis, that follows below, is possible if we consider the planes 3 and 4; see Fig. 1(a)].

Hence, the net ionic current density difference between both planes is $\Delta j = j_{2,+} - j_{1,+} = j_{1,-} - j_{2,-}$ (for detail expressions see the Supplemental Material [14]). From the analysis provided in [14] it is clear that due to the contribution of the DNA countercharge, Δj is always finite and positive [e.g., for 0.1 M salt concentration, $\Delta j/j = 0.0068$ and 0.0124 for nanochannel ($2H = w = 10$ nm) and nanopore ($R = 5$ nm), respectively, ensuring ion depletion in between planes 1 and 2 and enrichment in between planes 3 and 4, both in the nanochannel and the nanopore [see Figs. 1(a) and 1(c)].

We next attempt to obtain explicit 1D (axial) unsteady ion-distribution in the CP depletion zone. Therefore, the following analysis is identical for the nanochannel and the nanopore. We consider the location of plane 2 as $x = 0$, with the x axis being directed towards plane 1, see Figs. 1(a) and 1(c). The governing equation for the ionic transport (without electroosmotic advection) is

$$\partial c_i/\partial t = -\partial j_i/\partial x, \tag{1}$$

where j_i is the flux of the species i, given as $j_i = -D_i \partial c_i/\partial x + \mathrm{sgn}(z_i) c_i \mu_i E$. Here, c_i, D_i, μ_i, and z_i are the concentration (in M), diffusivity, mobility (unsigned) and valence, respectively, of species i. For the description of the electric field in the region between the planes 1 and 2, one can employ the Poisson equation in a formulation that relates the electric field to the constant current density j [15]:

$$\gamma E(x) + \varepsilon \partial E(x)/\partial t = j + F \sum_{i=1}^{N} z_i D_i \partial c_i/\partial x, \tag{2}$$

where ε is the permittivity of water and γ is the conductivity expressed as $\gamma = 10^3 F \sum_{i=1}^{N} |z_i| \mu_i c_i$. (1) and (2) are numerically solved (the results will be discussed later) first for $j = 0$ to obtain the equilibrium axial EDL, and then for a finite j using suitable initial and boundary conditions (for more details on the simulation, kindly refer to the legend of Figs. 3 and 4 and Refs. [16,17]). The DNA is present as a nondiffusing ionic species between (or at either sides of) planes 2 and 3 [see Figs. 1(a) and 1(c)] or in a concentration that in equilibrium yields the current transport numbers [18] for the mobile ions in accordance with the DNA-EDL model described above.

A closed form analytical solution of (1) and (2) for a 1:1 salt with ionic concentrations c_+ and c_- and equal ionic diffusivity D is

$$c_\pm(t, x > 0) = c_\infty - (j\Delta\Lambda_\pm/2FD)[2\sqrt{Dt/\pi} e^{-(x^2/4Dt)} - x\,\mathrm{erfc}(x/2\sqrt{Dt})], \tag{3a}$$

$$c_\pm(t, x > 0) = c_\infty - (j\Delta\Lambda_\pm/2FD)[2\sqrt{Dt/\pi} e^{-(x^2/4Dt)} + x\,\mathrm{erfc}(x/2\sqrt{Dt})]. \tag{3b}$$

Here, $\Delta\Lambda_i$ is the difference in transport numbers of species i between the positive and negative x regions, defined as $\Delta\Lambda_i = |\Lambda_i^{x<0} - \Lambda_i^{x>0}|$, where for all x $\Lambda_i = \langle c_i \rangle \mu_i / \sum_i \langle c_i \rangle \mu_i = \langle c_i \rangle D_i / \sum_i |z_i| \langle c_i \rangle D_i$. For detailed derivation as well as the meaning of the different quantities in (3a) and (3b) kindly see the supplemental material [14]. Analytical solutions in (3a) and (3b) are identical to that provided for a similar ion-depletion problem [19]. From (3a) and (3b), we can calculate the depletion time τ_S, or the time at which $c_\pm(x \to 0^+) = c_\pm(x \to 0^-) \to 0$ [16] as

$$\tau_S = (\tau_{S,+} + \tau_{S,-})/2 = (\pi 10^6 D F^2 c_\infty^2/j^2)(1/\Delta\Lambda_\pm)^2 \approx (\pi 10^6 R^2 T^2/DF^2E^2)(1/\Delta\Lambda_\pm)^2. \tag{4}$$

τ_S represents the time needed for maximum possible depletion—the smaller its value the more severe the CP effects. Figure 2, which is the central result of this Letter, shows the analytical solution for τ_S for different values of EDL-independent constant current density j_0 (j_0 is related to the electric field as $j_0 = 2 \times 10^3\ \mu\mathrm{FE}c_\infty$). In Fig. 2, we also provide a variation of the time scale of DNA electrophoretic motion; when $l_{\mathrm{pore/channel}} \gg l_{\mathrm{DNA}}$ (typically for a nanochannel, l denoting length) this represents the time the DNA travels its own length, $\tau_{\mathrm{DNA}} = \tau^c_{\mathrm{DNA}} = l_{\mathrm{DNA}}/\mu_{\mathrm{DNA}}E$ (where μ_{DNA} is the mobility of the DNA molecule) and when $l_{\mathrm{pore/channel}} \ll l_{\mathrm{DNA}}$ (typically for a nanopore) this represents the time in which the DNA partially fills the pore, $\tau_{\mathrm{DNA}} = \tau^p_{\mathrm{DNA}} = l_{\mathrm{pore}}/\mu_{\mathrm{DNA}}E$. Figure 2 summarizes the relevant system parameter space over which DNA-EDL induced CP affects DNA translocation, namely, when $\tau_S < \tau^c_{\mathrm{DNA}}$ or $\tau_S < \tau^p_{\mathrm{DNA}}$. Employing j_0 to obtain the electric field that governs τ^c_{DNA} or τ^p_{DNA} and assuming $j \sim j_0$, we get $\tau_S/\tau^{c/p}_{\mathrm{DNA}} \sim 1/j_0$, illustrating that at large current density (or equivalently at large electric fields), $\tau_S < \tau^{c/p}_{\mathrm{DNA}}$, ensuring that CP will be significant.

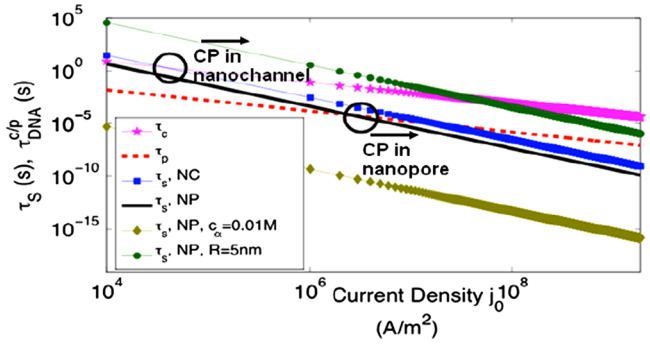

FIG. 2 (color online). Variation of τ_S and $\tau^{c/p}_{\mathrm{DNA}}$ [we denote τ^c_{DNA} as τ^c and τ^p_{DNA} as τ^p and take $l_{\mathrm{DNA}} = 10.0\ \mu$m ($l_{\mathrm{pore}} = 20.0$ nm) and $\mu_{\mathrm{DNA}} = 10^{-9}$ m^2/Vs] with applied average current density j_0 (defined as $j_0 = 2 \times 10^3\ \mu\mathrm{FEc}_\infty$) for different ionic concentrations and nanochannel or nanopore dimensions (here NC refers to nanochannel and NP refers to nanopore). Also, except where it is mentioned we take $c_\infty = 1$ M and R (or H) $= 1.25$ nm. The different constant parameters are $D_+ = D_- = D = 2 \times 10^{-9}$ m^2/s, $\mu_+ = \mu_- = \mu = 8 \times 10^{-8}$ m^2/Vs, $\zeta_w = -10$ mV, $q_B = 4$, and $\sigma = (2.4 \times 10^4/1.8 \times 10^{-5})$ e/m.

In Fig. 2 we see that CP will occur in a nanopore of 2.5 nm diameter above $j_0 = 5 \times 10^6$ A/m^2, or above 3.3×10^5 V/m in 1 M KCl (6 mV bias over a 20 nm pore). It is therefore certainly expected at the typical fields of $E \cong 10^7 - 10^8$ V/m [9]. The DNA-EDL ensures a finite value of the transport number differences $\Delta\Lambda_\pm$, and accordingly the parameters which will dictate $\Delta\Lambda_\pm$ are DNA-EDL cross sectional area and the DNA zeta potential; i.e., we may write $\Delta\Lambda_\pm \propto \lambda_D^2(ez\zeta_{\mathrm{DNA}}/k_BT)$, so that using the fact that $\lambda_D \sim 1/\sqrt{c_\infty}$ [20], we can obtain from (4) $\tau_S \sim c_\infty^4$ (see Fig. 2). Also for larger R, the relative effect of the DNA-EDL cross sectional area is reduced, thereby increasing the depletion time (see Fig. 2).

Figure 3(a) shows both the simulated as well as the analytical [see (3a) and (3b)] ionic concentration at $x = 0$ at the intermediate current density of 1.5×10^4 A/m^2. Simulations predict a quicker depletion, attributed to the ionic depletion at plane 2, which enhances $\Delta\Lambda-$ an effect not represented in (3a) and (3b). Figure 3(b) gives the simulated axial ionic concentration profiles, showing depletion and accumulation at opposite sides of the DNA. The simulations further show that the complete depletion, as predicted by (3a) and (3b), never occurs; rather a continuously growing extended space charge region is formed in front of the DNA. In this region, the space charge density as well as the final electrolyte concentration were found to increase with the current density, as visible in Figs. 3(c) and 3(d) (obtained for a current density of 1.5×10^6 A/m^2). Formation of such layers is described in literature on membrane CP [21].

Figures 4(a) and 4(c) provide the simulation results for the nanopore translocation of an entering and an exiting DNA, clearly indicating the ion depletion in front of the entering DNA and ion accumulation at the rear of the exiting DNA (note that the DNA moves opposite to the direction of the electric field). Figures 4(b) and 4(d) show that the typical depletion/accumulation time scale at the applied field is 1 to few nanoseconds. In this time the DNA (having a speed of $\mu_{\mathrm{DNA}}E \sim 0.1$ m/s) only moves subnanometer distances, so that the DNA can be approximated to be stationary during the ion depletion or accumulation events. More importantly, it is because of such extremely small time scale that CP has been yet to be reported in experimental studies of nanopore translocation driven DNA sequencing, where the achievable current resolution is about 100 μs. Branton *et al.* [10] state that in future the spatiotemporal current resolution must be drastically improved to allow single base-pair sequencing. For such cases we expect that CP will be clearly observed and it will be possible to quantify the effect of CP in the sequencing event.

CP-induced depletion and accumulation will alter the trans-pore conductance, in addition to the conductance alteration induced by the blockage effect of the DNA. For the example shown in Fig. 4 and for an open-pore conductance of 1, simulation results showed the conductance of a pore completely blocked by DNA is 0.42, that of a pore where an entering DNA blocks 1/3rd of the pore length is 0.36 and that of a pore where exiting DNA blocks 1/3rd of the pore length is 1.17. Such conductance values

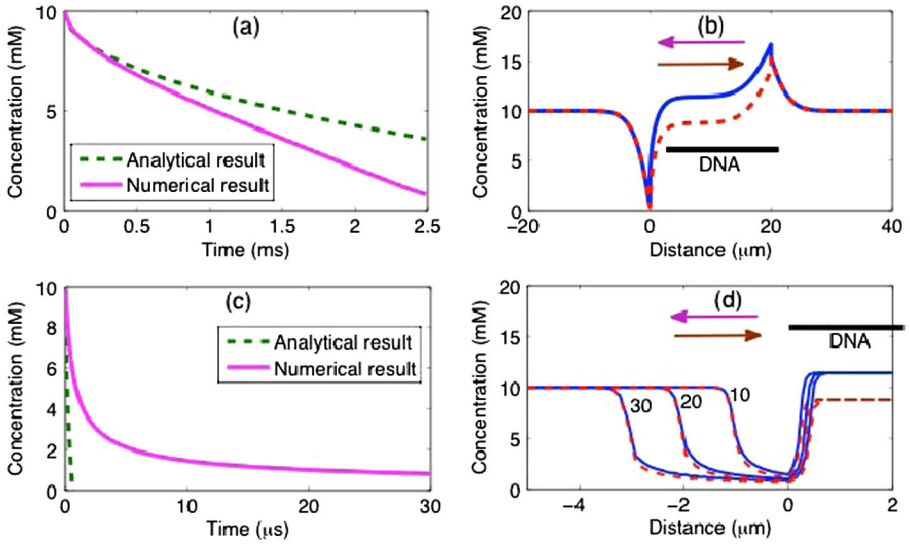

FIG. 3 (color online). (a),(c): Analytical and numerical simulation results for electrolyte depletion just outside the axial DNA EDL (at $x = -5\lambda_D$) in a 30×30 nm nanochannel with 10 mM KCl (K^+ are the cations and Cl^- are the anions) for (a) $j_0 = 1.508 \times 10^4$ A/m^2 and (c) $j_0 = 1.508 \times 10^6$ A/m^2. (b)(,d): Numerical simulation results for anionic (red dotted line) and cationic (blue bold line) concentration distributions for (b) $j_0 = 1.508 \times 10^4$ A/m^2 and $t = 2.5 \sim$ ms and (d) $j_0 = 1.508 \times 10^6$ A/m^2 and $t = 10$, 20, 30 μs (the numbers adjacent to the profiles denote the corresponding time in μs). For the corresponding average electric fields see caption of Fig. 2. In (b) and (d), the purple arrow indicates DNA movement direction and the brown arrow applied field direction. Also in these figures we denote the location of DNA by a black line. The different parameters used for the analytical calculations are as in Fig. 2. For the numerical calculations, in addition to these parameters, we consider an immobile (negative) charge concentration of 2.628 mM over a length of 20 μm (typical for λ-DNA stretched in a 30×30 nm channel).

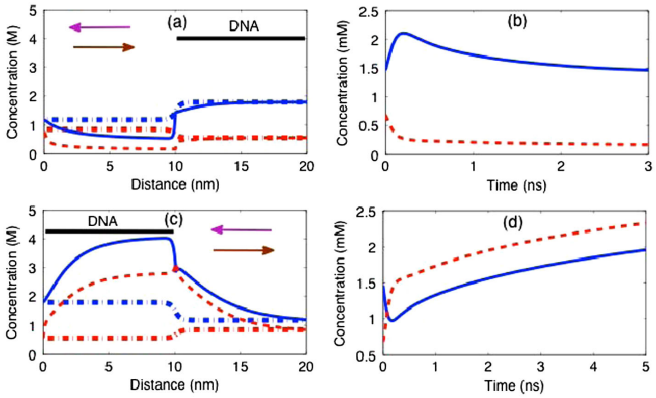

FIG. 4 (color online). Numerical simulation results for cation and anion distribution in a nanopore for (a) an entering DNA at $t = 10$ ns after current application and (c) an exiting DNA at $t = 100$ ns after current application. Blue bold lines and red dashed lines depict the cation and anion concentrations, respectively, at $t = 10$, 100 ns and dash-dotted lines the cation (blue) and anion (red) concentrations at $t = 0$ (i.e., before current application). Numerical simulation results for temporal variation of cation (blue bold lines) and anion (red dashed lines) concentrations at $x = 10$ nm are shown in (b) and (d). In (b) this location is in front of the DNA and in (d) at the back of the DNA. In figs. (a) and (c), the purple arrow indicates DNA movement direction and the brown arrow applied field direction. The location of the DNA is indicated by a black line. We also use $R = 1.25$ nm, $j_0 = 1.508 \times 10^9$ A/m^2 (initial field $\sim 10^8$ V/m), DNA length = 10 nm, pore length = 20 nm (the corresponding bias voltage will therefore be 2 V). At the DNA section the immobile (negative) charge concentration is equal to 1232.4 mM, whereas that at the bare channel section is equal to 330.836 mM. At the pore ends bulk concentrations (1000 mM) exist.

above the open-pore value (for an exiting DNA) and below the blocked pore value (for an entering DNA) have been witnessed in several molecular dynamics simulation studies [3,4,9] without emphatic justification—therefore our paper by hypothesizing that CP is responsible for such effects provides the first concrete justification for such strongly nontrivial translocation current signatures. Also in experimental results involving nanopore translocation of HP DNA distinct current peaks have been observed, although the corresponding current dips are absent [4]. This can be associated to the fact that the extent of current dips are less prominent than the current spikes [e.g., in the numerical example corresponding to Fig. 4 that we provide above, the dip is equivalent to lowering of the fully blocked pore conductance by 6%, whereas the spike is equivalent to the increase of the fully open-pore conductance by 17%].

Note that only for the 1-D DNA translocation cases (i.e., translocation in thin nanochannels and nanopores), the CP-nullifying diffusion current can decay to zero (over a time scale $\tau_D \sim (Fc_\infty D/j_D)^2 \sim D/\mu^2 E^2$) [22]. In contrast, however, in microchannel DNA electrophoresis, which is effectively a 3-D system, the CP-nullifying diffusion current never completely decays [22], thereby substantially neutralizing the impact of CP. Therefore one will expect significant CP only during nanopore or nanochannel (and not microchannel or gel) DNA electrophoresis.

To summarize, we have demonstrated that large electric field translocation of a single nanoconfined DNA molecule leads to strong CP effects causing ion depletion and ion enrichment at the front and the rear ends of the DNA molecule (please see [23] for some preliminary experiments). As the phenomenon strongly affects the local conductivity, it becomes especially relevant for nanopore DNA sequencing methods that rely on such conductance changes [10,17]. One possible approach considered to enable sequencing is to slow down the DNA by increasing its friction with the pore, while applying a sufficiently strong field to ensure a measurable current [10]—for such a case CP will readily evolve. It is therefore important to stress the relevance of CP in design and measurement of future nanopore-based DNA sequencing devices. In addition, our theory shows how CP can explain several nontrivial current signatures in form of sharp spikes and dips observed (but unexplained) in molecular dynamics simulation studies of nanopore DNA translocation or experimental studies of nanopore HP DNA transport.

[1] C. Dekker, Nature Nanotech. **2**, 209 (2007); F. Baldessari and J. G. Santiago, J. Nanobiotech. **4**, 12 (2006).
[2] B. Luan and A. Aksimentiev, J. Phys. Condens. Matter **22**, 454123 (2010).
[3] A. Aksimentiev, Nanoscale **2**, 468 (2010).
[4] J. Comer *et al.*, Biophys. J. **96**, 593 (2009).
[5] Q. Zhao *et al.*, Nucleic Acids Res. **36**, 1532 (2008).
[6] G. B. Salieb-Beugelaar *et al.*, Nano Lett. **8**, 1785 (2008).
[7] H. Strathmann, J. Membr. Sci. **9**, 121 (1981).
[8] S. J. Kim *et al.*, Chem. Soc. Rev. **39**, 912 (2010).
[9] A. Aksimentiev *et al.*, Biophys. J. **87**, 2086 (2004).
[10] D. Branton *et al.*, Nat. Biotechnol. **26**, 1146 (2008).
[11] R. M. M. Smeets *et al.*, Nano Lett. **6**, 89 (2006).
[12] J. B. Heng *et al.*, Biophys. J. **87**, 2905 (2004).
[13] R. Karnik *et al.*, Nano Lett. **7**, 547 (2007).
[14] See Supplemental Material at http://link.aps.org/supplemental/10.1103/PhysRevLett.108.138101 for details.
[15] T. R. Brumleve and R. P. Buck, J. Electroanal. Chem. **90**, 1 (1978).
[16] O. M. Bockris and A. K. N. Reddy, *Modern Electrochemistry* (Kluwer Academic/Plenum Publishers, New York, 1998).
[17] M. Fyta *et al.*, Pol. Phys. **49**, 985 (2011).
[18] D. J. Dewhurst, Trans. Faraday Soc. **56**, 599 (1960).
[19] M. van Soestbergen, P. M. Biesheuvel, and M. Z. Bazant, Phys. Rev. E **81**, 021503 (2010).
[20] R. J. Hunter, *Zeta Potential in Colloid Science* (Academic Press, London, 1981).
[21] I. Rubinstein and L. Shtilman, J. Chem. Soc., Faraday Trans. 1 **75**, 231 (1979).
[22] K. Aoki, Electroanalysis **5**, 627 (1993).
[23] Y-H. Shen and R. Karnik, *25th IEEE Conference on MEMS 2012*, Paris, France.